Tracking the Evolution of Interatomic Potentials with High Resolution Inelastic Neutron Spectroscopy

J. Z. Larese,[1,*] D. Martin y Marero,[2] D. S. Sivia,[2] and C. J. Carlile[2,3]

[1]*Chemistry Department, Brookhaven National Laboratory, Upton, New York 11973*
[2]*ISIS, Rutherford Appleton Laboratory, Didcot, United Kingdom*
[3]*Institut Laue Langevin, Grenoble, France*

(Received 27 October 2000; published 26 October 2001)

High resolution inelastic neutron scattering has been used to characterize the low temperature rotational dynamics of methane (CH_4) films on MgO(100) surfaces as a function of layer thickness. At low temperatures the films grow layer-by-layer similar to the (100) planes of bulk solid CH_4. We observe a crossover in the CH_4 tunneling spectrum from one characteristic of the 2D solid at monolayer coverages into one that is bulklike (i.e., 3D) when the film is six layers thick. These findings place significant constraints on the microscopic models used to describe CH_4-CH_4 and CH_4-MgO interactions.

DOI: 10.1103/PhysRevLett.87.206102 PACS numbers: 68.43.–h, 61.12.Ex, 68.47.Gh

Although neutrons interact only weakly with matter, elastic and inelastic neutron scattering (INS) are excellent methods for examining the structure and dynamics of films adsorbed on solid surfaces. The sensitivity of INS methods to characterize the low temperature quantum reorientation in molecular solids is unrivaled [1,2]. Furthermore, a recent study of the rotational dynamics in CH_4 clathrates [3] illustrates that INS methods are extremely useful for understanding and *quantitatively* describing intermolecular interactions.

In this Letter we describe how synthetic, thermodynamic, and neutron scattering methods are combined to explore the evolution of molecule-molecule and molecule-substrate interactions. Changes in the inelastic neutron spectrum are used to show that the intermolecular interactions evolve as a CH_4 film grows from two to three dimensions. Furthermore, we show that these changes can be used to distinguish molecules near the substrate from those farther away.

The interaction of CH_4 with MgO surfaces has been the subject of numerous studies. Methane exhibits interesting adsorption and layering properties on MgO. Since MgO is catalytically active, much effort has centered on understanding how it promotes the production of methanol and other higher hydrocarbons from CH_4. From a fundamental perspective, interest has concentrated on developing accurate theoretical descriptions of the CH_4-MgO interaction and a quantum description of the hindered rotor motion. Todnem *et al.* [4] and Picaud and co-workers [5] summarize the current understanding.

Press and Kollmar were first to measure the rotational tunneling spectrum of phase-II solid CH_4 [6]. They found that three-fourths of the molecules in this phase were orientationally ordered, while one-fourth of the molecules freely rotated within the solid. Hüller and Kroll (HK) [7] refined the method of Nagamiaya [8] for describing the ground state rotational level diagram for tetrahedral molecules in fields of different symmetry [Fig. 1(a)]. HK showed that, when the phase-II CH_4 solid forms, the degeneracy of the T state remains.

The HK concepts and earlier neutron diffraction studies [9] led us to believe that a monolayer film of CH_4 on MgO would be a good candidate for observing a significant splitting of the rotational T state. Hence, nearly a decade ago, employing the best MgO powders available *at the time,* we used INS techniques to measure the tunneling spectrum of a monolayer film of CH_4 on MgO(100) surfaces [10]. We used symmetry arguments to show that at low temperature CH_4 forms an ordered solid on the MgO surface, with the C_{2v} axis of the molecule normal to the surface plane. This suggests that the interaction potential of CH_4 with the MgO(100) surface is very different from that in the bulk phase-II solid or when isolated in rare-gas solids [11] or adsorbed on graphite [12].

Subsequently, significant improvements have been made in our MgO synthesis technique [13,14]. Figure 1(b) shows our recent INS measurements of monolayer CH_4 films using the IRIS spectrometer at the ISIS pulsed source [15]. The solid line is a numerical fit made with the Bayesian data analysis package developed for use with the IRIS spectrometer by Sivia and Carlile [16], which results in a spectrum composed of eight lines. Table I compares the line positions calculated using the best theoretical model currently available for tetrahedral molecules (see Ref. [10]) with those found by the Bayesian fit. The excellent agreement between the model predictions and Bayesian analysis illustrates that for monolayer films of CH_4 on MgO the molecules predominantly sit with their C_{2v} axes normal to the MgO(100) plane [Fig. 1(b) inset].

As part of our ongoing effort to investigate the structure and dynamics of molecular adsorption going from two to three dimensions, we employed INS techniques to probe the development of intermolecular interactions as a function of layer thickness. Our adsorption isotherms [14] and earlier neutron diffraction studies by Gay and co-workers [17] indicate that CH_4 films grow in a layer by

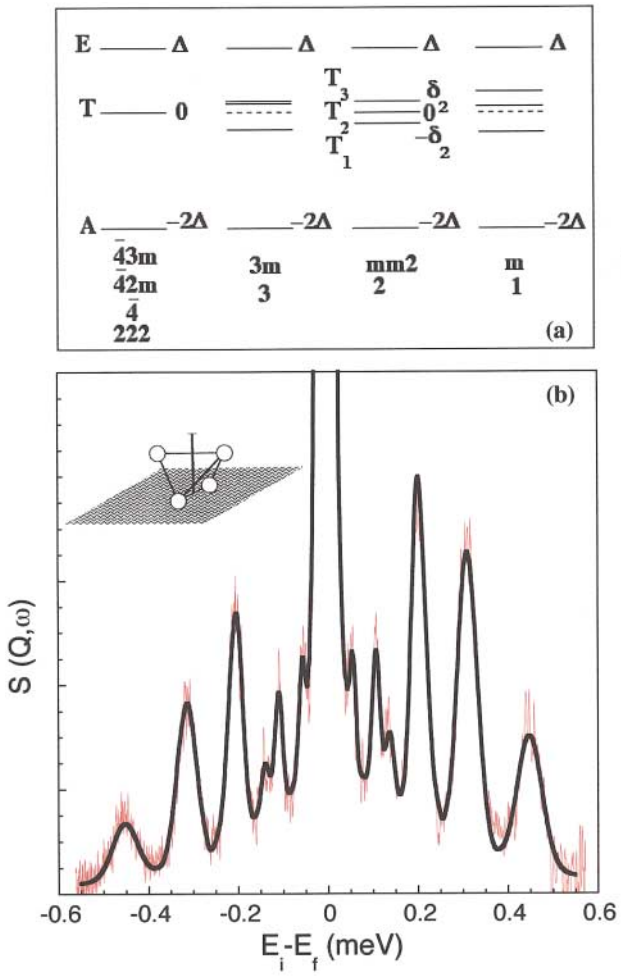

FIG. 1 (color). Tunneling splitting of the librational ground state of a CH_4 molecule in fields of different symmetry. The ($\bar{4}3m$) diagram applies to CH_4-II solids, while ($mm2, 2$) was used to model the monolayer CH_4/MgO spectrum. (b) INS tunneling spectrum of a 0.9 layer of CH_4 on MgO at 1.5 K using IRIS (energy resolution ~17 μeV, FWHM). The solid line is a Bayesian fit to the data as described in Ref. [16]. The inset illustrates the C_{2v} orientation of CH_4 on MgO(100).

layer fashion on MgO-like successive (100) planes of the fcc, phase-II solid CH_4. Because the C_{2v} symmetry of the monolayer solid removes the degeneracy of the T state, it is reasonable to assume that the spectrum presented in Fig. 1(b) is an appropriate signal to follow the evolution of the rotational potential as a function of CH_4 coverage. Figure 2 shows the observed spectral changes as a function of layer thickness. The lowest (uppermost) trace is a spectrum recorded from a monolayer (six-layer) film. The arrows indicating the locations of CH_4-II $A \rightarrow T$ and $T \rightarrow E$ transitions come from data recorded by Asmussen *et al.* [18]. Several comments are in order. First, there is a dramatic change in the number and sharpness of the spectral features comparing the one- and two-layer films. Beyond that, however, there is a relatively smooth evolution of the inelastic response as a function of coverage, as evidenced by the much less

TABLE I. Comparison of model calculations (Ref. [10]) with fits to data in Fig. 1(b) using Bayesian analysis. Model calculations use molecule-to-surface distance of 3.30 Å and molecular field of 21.8 cm^{-1} and level diagram ($mm2, 2$).

Transition	Model (μeV)	Experiment (μeV)
$E \rightarrow T3$	59	56.6 ± 0.5
$T2 \rightarrow T1$	110	108.2 ± 0.4
$T3 \rightarrow T2$	134	139.7 ± 0.7
$E \rightarrow T2$	193	200.0 ± 2.1
$T1 \rightarrow A$	212	218.0 ± 3.7
$T3 \rightarrow T1$	Not Allowed	Not Observed
$E \rightarrow T1$	300	306.2 ± 0.4
$T2 \rightarrow A$	322	324.0 ± 2.5
$T3 \rightarrow A$	456	450.4 ± 0.7

dramatic change in the inelastic spectrum from two to three layers. Figure 1(a) illustrates that the main effect of adsorption site symmetry on the rotational ground state manifold is the extent to which the T state is split. Second, beyond four layers the spectrum takes on the overall appearance of the bulk CH_4 spectrum. Further increases in film thickness result in spectra that grow more intense and narrower in width, and converge (in energy and width) toward the bulk CH_4 phase-II solid spectrum. The inelastic signals presented here from films 4—6 layers thick are not

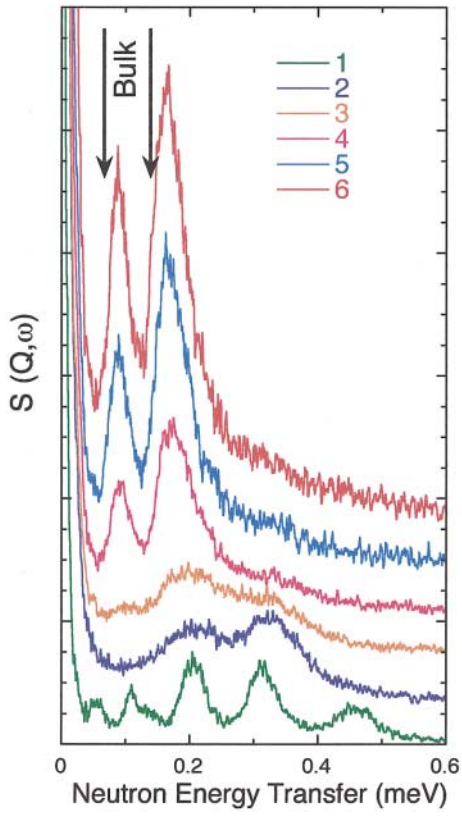

FIG. 2 (color). INS tunneling spectra of CH_4 on MgO at 1.5 K as a function of film thickness. Curves from bottom to top represent nominal coverages of 1, 2, 3, 4, 5, and 6 layers. Arrows mark the $T \rightarrow E$ and $A \rightarrow T$ transitions for CH_4-II.

the same as those recorded when small bulk CH_4 crystallites form. We intentionally created small crystallites by rapidly cooling a cell filled with enough CH_4 to form a four-layer film. The resulting spectrum was narrow in shape [full width at half maximum (FWHM) = 17 μeV, and positioned at energy transfer values (75 and 145 μeV) identical to those in the bulk CH_4-II solid superposed on a broad symmetric background. This was never observed in the experiments using uniformly prepared and annealed CH_4 films. Third, the changes observed in the tunneling spectrum are directly related to the evolution of the CH_4-CH_4 and CH_4-MgO interaction potentials. In principle, modeling the layering behavior described here should be less ambiguous than modeling of matrix-isolated molecular tunneling. The structure of the solid adsorbed film is well defined, whereas the local structure in the matrix-isolation studies can only be described statistically.

Additional information concerning the interaction potentials is also obtained by examining the inelastic response of the CH_4-MgO system at larger energy transfers. We noted above that, for bulk phase-II solid CH_4, one-fourth of the molecules rotate freely. Thus at energy transfers near 1.1 meV the $0 \rightarrow 1$ free rotor transition is observed. Figure 3 shows the coverage dependence of the inelastic response of the CH_4 on the MgO system in the 0.75–1.2 meV range. At monolayer coverage *no feature* is observed in this energy transfer range, whereas in the bulk CH_4 spectrum the free rotor $0 \rightarrow 1$ transition is readily observed (at approximately 1.06 meV). At CH_4 coverages between one and two layers, however, two well-defined features appear near 0.88 and 0.96 meV. The bilayer spectrum of Fig. 3 was recorded close to layer completion (where some third-layer occupation is likely) and it is clear that three well-defined features appear in the spectrum, centered at 0.88, 1.0, and 1.09 meV. As the film thickness increases, the intensity of the spectrum near 1.1 meV grows while the features at lower energies broaden and move toward higher energies. A distinct asymmetry on the low energy side of the peak near 1.1 meV develops similar in shape to the $0 \rightarrow 1$ free rotor transition in bulk CH_4. The asymmetric broadening of the free rotor line is found in other molecular systems [19]. Small variations in the local structure and symmetry of the film result in variations in the rotational hindering potentials. There are two points worth noting: (i) The wing recorded in the adsorbed film system appears on the low energy transfer side of the 1.1 meV feature, and (ii) in the ideal (semiclassical) case of a completely isolated single CH_4 molecule a value of 1.3 meV is predicted for the $0 \rightarrow 1$ free rotor transition. Both facts indicate that neighboring molecules and the substrate act to increase the height of the local potential barrier of an isolated molecule and thereby hinder the "free" rotational motion.

We used a commercial energy minimization/modeling package from Molecular Simulations, Inc. [20] to examine

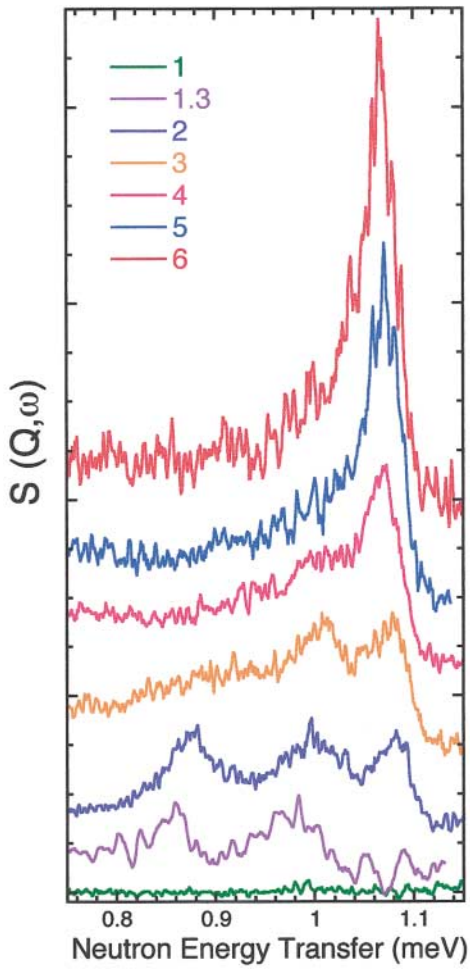

FIG. 3 (color). INS free rotor spectra of CH_4 on MgO at 1.5 K as a function of film thickness. Spectra are ordered and labeled the same as Fig. 2, except for 1.3 layers.

the rotational properties of CH_4 molecules on the MgO surface. The program uses a universal force field, first described by Rappé *et al.* [21] and shown to work for organic molecules by Casewit *et al.* [22], to model the intermolecular interactions. We studied how the rotational barrier of the single CH_4 molecule on the MgO surface is different from that of an individual molecule within a small patch of molecules (i.e., a 5×5 cluster of molecules created by placing nearest neighbors and next-nearest neighbors at the $\sqrt{2} \times \sqrt{2}$ R 45° distance) on the MgO(100) surface. We also explored how the rotation barrier varies individual molecules residing at different layers within a multilayer slab of commensurate molecules assembled to mimic the (100) face of a cubic CH_4 crystal (from two to several layers thick). To determine how the rotational barrier height changed we used the following method. Initially in each run all the molecules were placed in their original commensurate positions and dipod (ferro) orientations. Then a "probe" molecule was randomly reoriented and then fixed in its new position. The energy of the ensemble was minimized by allowing the local

molecular environment to respond freely to the new (but fixed) orientation of the probe molecule. This procedure was repeated numerous times so that an estimate of a potential well could be derived. While it is difficult to assign quantitative values for the resulting potential barriers several observations can be made. Molecules in the layer closest to the MgO substrate are significantly less likely (about a factor of 2 greater well depth) to exhibit free rotation (either in isolation or within a small ordered cluster). Molecules in layers farther from the surface feel a decrease in rotational hindrance as their distance from the MgO surface increases (largely in response to the nominal r^{-3} decrease in the attractive part of the molecule-substrate potential). Finally, when the film thickness exceeds three or four layers, molecules within the outer layers of these solid slabs experience roughly the same hindering potential (the well depth varies by only 5%–10% beyond layer three). This suggests that the CH_4-CH_4 interactions dominate in the layers farthest from the surface. If we assume an exponential relationship between the potential well for the first and second layers and the position of the nearly free rotor, $\hbar\omega_A = \hbar\omega_{\text{free rotor}} \exp(-V^2/2\Gamma^2)$ [23], the experimental data can be used to obtain a ratio of the barrier heights for the hindered rotor states near 1 meV. Such a procedure indicates that the ratio of the hindered rotor barriers $\hbar\omega_A/\hbar\omega_B \sim 0.65$. We used $\hbar\omega_{\text{free rotor}}$ as the free rotor transition (1.31 meV) and estimated $\hbar\omega_A$, $\hbar\omega_B$ from the two inelastic peaks near 0.85 and 1.0 meV, respectively, in trace 1.3 in Fig. 3. Based upon these findings we conjecture that the multiple peaks observed in the one to three-layer films result from molecules that reside in different layers close to the MgO substrate. We suspect that there is a reduction in the hindering potential (rotational barrier) for molecules in the first layer once molecules start to occupy the second layer. This results in the two sharp transitions observed near 1 meV. This behavior is likely to be a direct response to the interlayer CH_4-CH_4 interaction and is consistent with the hindered rotor behavior suggested by Picaud *et al.* [5].

The results presented above illustrate that INS is a useful tool for observing the crossover in behavior from two to three dimensions and for probing the development of interaction potentials in multilayer film systems. Futhermore, we present evidence for site and thickness dependent free rotor barriers. These results place certain restrictions on a theoretical description of the interaction of CH_4 with MgO. An accurate model must predict (*i*) a significant barrier to "free rotation" for monolayer films, i.e., the absence of the $0 \rightarrow 1$ free rotor transition; (*ii*) an evolution of the molecule-substrate potential so that free rotorlike motion occurs once molecules occupy the second layer and beyond; (*iii*) that CH_4 films grow layer-by-layer on MgO(100) similar to the (100) face of bulk CH_4. *Ab initio* quantum methods that address multilayer tunneling have yet to be developed, but recent theoretical efforts by Ozaki [24] are encouraging.

We thank B. Asmussen, A. Freitag, L. Daemen, J. M. Hastings, W. Kunnmann, A. Novaco, L. Passell, W. Press, M. Sprung, and D. Smith for useful discussions. Support was provided by the U.S. Department of Energy, Materials Science Division, under Contract No. DE-AC02-98CH10886.

*Current address: Chemistry Department, University of Tennessee, Knoxville, Tennessee.

[1] M. Bee, *Quasielastic Neutron Scattering* (Adam Hilger, Bristol, 1987), and references therein.
[2] W. Press, *Single-Particle Rotations in Molecular Crystals* (Springer, Berlin, 1981), and reference therein.
[3] C. Gutt *et al.,* Phys. Rev. B **59**, 8607 (1999).
[4] K. Todnem, K. J. Bourve, and M. Nygren, Surf. Sci. **421**, 296 (1999).
[5] S. Picaud, C. Girardet, T. Duboo, and D. Lemoine, Phys. Rev. B **60**, 8333 (1999).
[6] W. Press and A. Kollmar, Solid State Commun. **17**, 405 (1975).
[7] A. Hüller and D. M. Kroll, J. Chem. Phys. **63**, 4495 (1975).
[8] T. Nagamiaya, Prog. Theor. Phys. **6**, 702 (1951).
[9] J. P. Coulomb *et al.,* Phys. Rev. Lett. **54**, 1536 (1985).
[10] J. Z. Larese *et al.,* J. Chem. Phys. **95**, 6997 (1991).
[11] M. Prager, B. Asmussen, and C. J. Carlile, J. Chem. Phys. **100**, 247 (1994), and references therein.
[12] A. Inaba *et al.,* J. Chem. Phys. **103**, 1627 (1995).
[13] J. Z. Larese and W. Kunnmann (U.S. Patent No. 6 179 897).
[14] A. Freitag and J. Z. Larese, Phys. Rev. B **62**, 8360 (2000).
[15] C. J. Carlile and M. A. Adams, Physica (Amsterdam) **182B**, 431 (1992).
[16] D. S. Sivia and C. J. Carlile, J. Chem. Phys. **96**, 170 (1992).
[17] J. M. Gay, J. Suzanne, and J. P. Coulomb, Phys. Rev. B **41**, 11 346 (1990).
[18] B. Asmussen *et al.,* J. Chem. Phys. **97**, 1332 (1992); B. Asmussen *et al., ibid.* **103**, 221 (1995).
[19] F. Fillaux, C. J. Carlile, and G. J. Kearley, Phys. Rev. B **58**, 11 416 (1998).
[20] Cerius$^{2®}$ Software, Molecular Simulations, Inc., San Diego, California, 92121, U.S.A.
[21] A. Rappé, C. Casewit, K. Colwell, W. Goddard, and W. Skiff, J. Am. Chem. Soc. **114**, 10 024 (1992).
[22] C. Casewit, K. Colwell, and W. Goddard, J. Am. Chem. Soc. **114**, 10 035 (1992).
[23] B. Asmussen *et al.,* J. Chem. Phys. **98**, 158 (1993).
[24] Y. Ozaki (private communications); (to be published).